ELSEVIER

Journal of Marine Systems 6 (1995) 363–380

JOURNAL OF MARINE SYSTEMS

Thermal forcing for a global ocean circulation model using a three-year climatology of ECMWF analyses

B. Barnier *, L. Siefridt, P. Marchesiello

Equipe de Modélisation des Ecoulements Océaniques et des Marées, Laboratoire des Ecoulements Géophysiques et Industriels, URA CNRS 1509, Institut de Mécanique de Grenoble, Grenoble, France

Received 25 February 1994; accepted 25 October 1994

Abstract

A surface thermal boundary condition for a world ocean model is proposed. The formulation is based on previous methods which have used bulk formulas to define a model-dependent correction to the air–sea fluxes applied to the model. An estimate of the flux correction is calculated from a recent 3-year climatology of atmospheric surface fields provided by the 6-hour analyses performed at the European Center for Medium-range Weather Forecasts. The mean correction term and its seasonnal cycle are analysed and compared to similar climatological quantities.

1. Introduction

There are several ways to formulate the thermal forcing of an Ocean General Circulation Model (OGCM). A formulation which attempts to remain close to the physics of air–sea interactions is the flux boundary condition. It is assumed that the upper ocean is heated by the downward penetration of the solar radiation according to a depth-dependent absorption law, and cooled by the non-solar heat flux at the air–sea interface. The advection–diffusion equation for the time evolution of the ocean temperature T,

$$\frac{\partial T}{\partial t} = \text{Advection} + \text{Diffusion} + F_{\text{SOL}}(z) \qquad (1a)$$

therefore includes a source term, $F_{\text{SOL}}(z)$, which represents the depth-dependent heating by the solar heat flux. $F_{\text{SOL}}(z)$ is commonly parameterised by an absorption law (Paulson and Simpson, 1977). The forcing of the ocean temperature by the non-solar heat flux Q_{NS} (the addition of the net infra-red, latent and sensible heat fluxes) is introduced as a surface boundary condition:

$$\left(K_V(z)\frac{\partial T}{\partial t}\right)_{z=0} = \frac{Q_{\text{NS}}}{\rho_0 C_{P\text{w}}} \qquad (1b)$$

where K_V is a mixing coefficient that depends on depth. Other parameters are defined in the Appendix. This type of formulation is commonly used for mixed-layer models (Gaspard et al., 1990). Numerical stability of this flux boundary condition requires a fine vertical grid near the surface and knowledge of $K_V(z)$ at the surface.

In a slightly different formulation often used in OGCM, the solar heating is not modelled according to a depth-dependent penetration law as in Eq. (1a), but is introduced via the surface flux boundary condition Eq. (1b) which is formu-

* Corresponding author.

SSDI 0924-7963(94)00034-4

lated with the net heat flux Q_{NET}. This assumes that the solar heat flux is totally absorbed between the surface and the first vertical level of the model.

However, in the case of a low vertical resolution, the flux boundary condition may not be appropriate, and a "body force" parameterisation can be used which consists of a source term F in the temperature equation applied over a finite pre-defined depth Δz (the Ekman layer depth for example). The temperature equation at the vertical levels between the surface and Δz becomes:

$$\frac{\partial T}{\partial t} = \text{Advection} + \text{Diffusion} + F \qquad (2a)$$

The source term F can be formulated as a relaxation of the model temperature toward a climatological sea surface temperature T_S^{clim}

$$F = \frac{1}{R}\left(T_S^{clim} - T\right) \; 0 \le z \le \Delta z \qquad (2b)$$

where R is a relaxation constant (dimension of a time). This formulation has been used frequently (Cox and Bryan, 1984, Webb et al., 1991). It has the advantage of being independent of knowledge of $K_V(z)$ at the surface, but requires an estimate of the relaxation constant, often chosen in the range of 30 to 40 days.

The source term can be chosen to be proportional to the net surface heat flux:

$$F = \frac{Q_{NET}}{\rho_0 C_{Pw} \Delta z} \qquad (2c)$$

which means that, by unit time dt and over the depth, Δz the net surface heat flux uniformly modifies the ocean temperature by an amount $\Delta T = F \cdot dt$. This assumes a uniform and instantaneous vertical mixing of temperature from the surface to depth Δz.

All the above formulations, except Eq. (2b), require knowledge of the heat fluxes at the air–sea interface, estimates of which are obtained from analyses conducted at various meteorological centers such as the European Center for Medium-range Weather Forecasts (ECMWF) (Simonot and Le Treut, 1987; Barnier and Simonot, 1990), the National Meteorological Center (NMC) and other centers (Lambert and Boer, 1988), or various climatologies obtained from the Volunteer Observing Ship (VOS) data collection (Esbensen and Kushnir, 1981; Hsiung, 1986; Oberhuber, 1988). However, forcing an OGCM with specified heat flux estimates often results in an unrealistic Sea Surface Temperature (SST). For example, the attempt of Rosati and Miyakoda (1988) to drive an upper ocean global model with specified wind-stress and heat flux, showed that the SST predicted by the model could be significantly different from the climatological SST used in the calculation of the flux. In their analysis, they questioned the inconsistency of the climatological forcing (they noticed that low wind speed could be locally associated with high evaporation rates). However, the absence of interactivity between their ocean model and the atmosphere could also account for the drift of the model SST.

The ideal solution lies in coupling ocean and atmosphere models. Although recent progress has been made in that field, such studies carried out with low resolution models are still in their early stages, and it is still of prime interest to investigate the response of ocean models under the action of a prescribed atmosphere in order to understand the dynamics that drive the general circulation of the ocean.

A surface flux-type thermal boundary condition allowing for a coupling at large scales of an ocean model to a prescribed atmosphere was first proposed by Haney (1971). Based on a linear development of empirical surface heat flux formulas, Haney expressed the downward heat flux at the ocean surface as a relaxation term of the model ocean sea surface temperature (SST) to an equivalent air temperature which includes the effects of evaporation and solar radiation. Following the same approach, Takano et al. (1973) proposed a method which can be considered as intermediate before a fully coupled ocean–atmosphere model can be used. All surface heat flux components are computed (at model grid points) using empirical bulk formulas with specified climatological atmospheric parameters and oceanic variables from the ocean model. Han (1984) performed simulations of the world ocean circulation, focusing his interest on finding the states of the ocean which are in quasi-equilibrium with a

prescribed atmosphere. His surface thermal boundary condition essentially followed the method of Takano et al. (1973), but he developed a simplified formulation similar to that of Haney (1971). The major effect of the formulation of Han (1984) is to update the heat flux that forces the ocean model in such a way that the ocean circulation is driven toward a state of equilibrium with the prescribed atmosphere. It has been used since then in recent major eddy-resolving general circulation model (EGCM) simulations (Semtner and Chervin, 1988; Bleck et al., 1989; Bryan and Holland, 1989; Semtner and Chervin, 1992), as well as in recent studies investigating the role of the ocean in climate change (Weaver and Sarachik, 1991; Moore and Reason, 1993; Tziperman et al., 1994). These climate studies suggest that the meridional overturning circulation in the North Atlantic could undergo drastic modifications depending on the heat and fresh water flux conditions, many of the above studies relying on a fixed flux of salt as a boundary condition for the salinity equation. However, Huang (1993) argued that the salt flux is virtually zero in the real ocean, where it is the salt concentration which varies according to the evaporation rate or precipitation. He therefore proposed a natural boundary condition for the fresh water flux which keeps a zero flux of salt across the ocean surface. In recent sensitivity studies on the response of the overturning cell in the North Atlantic to surface boundary conditions, Holland and Bryan (1994) point out the importance of parameterising the heat flux which accounts for interactions with the atmosphere (since the heat flux in the real ocean is a function of the ocean surface temperature) and emphasize the difficulty of parameterising the fresh water flux, which is by nature independent of sea-surface salinity, but locally related to the heat flux through evaporation.

It is not the purpose of the present study to discuss the parameterisation of the fresh water flux in ocean models. The ideal boundary condition for the salinity equation has yet to be determined, and requires better knowledge of the precipitation field over the ocean. The best climatology of the precipitation over the ocean will probably come from analyses performed by Numerical Weather Prediction (NWP) centers such as ECMWF or NMC. One expects such analyses to ensure the consistency between evaporation, wind stress and latent heat flux. Therefore, it appears important to investigate the heat flux boundary condition that can be derived from meteorological data provided by the major NWP centers.

It should be also noted that, with a view to investigating the physical processes that are responsible for the present state of the ocean circulation, the World Ocean Circulation Experiment (WOCE) program supports global-scale and basin-scale eddy-resolving modelling studies attempting to simulate the quasi-equilibrium state of the ocean under a constant climatological atmospheric forcing. The major studies in this context (Semtner and Chervin, 1988 and Semtner and Chervin, 1992; The FRAM experiment: Webb et al., 1991; The CME experiment: Bryan and Holland, 1989, Böning and Herrmann, 1994, Holland and Bryan, 1994) show that there is still a clear need for better formulations and estimates of the atmospheric forcing, in particular in the Southern Hemisphere where VOS data are sparse.

Here we propose a flux-type surface thermal condition for EGCM's. Formulation is largely based upon the efforts of Haney (1971) and Han (1984), and calculations over the world ocean use a 3-year-seasonal climatology of ECMWF surface analyses.

The paper is organised into five sections. Following this introduction (Section 1), Section 2 describes the ECMWF data set from which the thermal forcing is calculated. Section 3 presents the formulation of the thermal forcing and the estimates of its various components obtained with ECMWF data. The total thermal boundary condition obtained over the world ocean with ECMWF data is analysed and compared with estimates from Han (1984) in Section 4. The seasonal cycle is briefly discussed in Section 5.

2. The ECMWF data set

The basic data are from the AVISO data set (Siefridt and Barnier, 1993) which includes many

surface variables available from the ECMWF data records. The mean sea level pressure, the sea surface temperature, the air and dew point temperatures at 2 m, and the wind vector at 10 m are obtained from the global analyses performed every 6 hours at ECMWF with a four dimensional data assimilation procedure (Bengtsson et al., 1982). The ECMWF model also calculates the

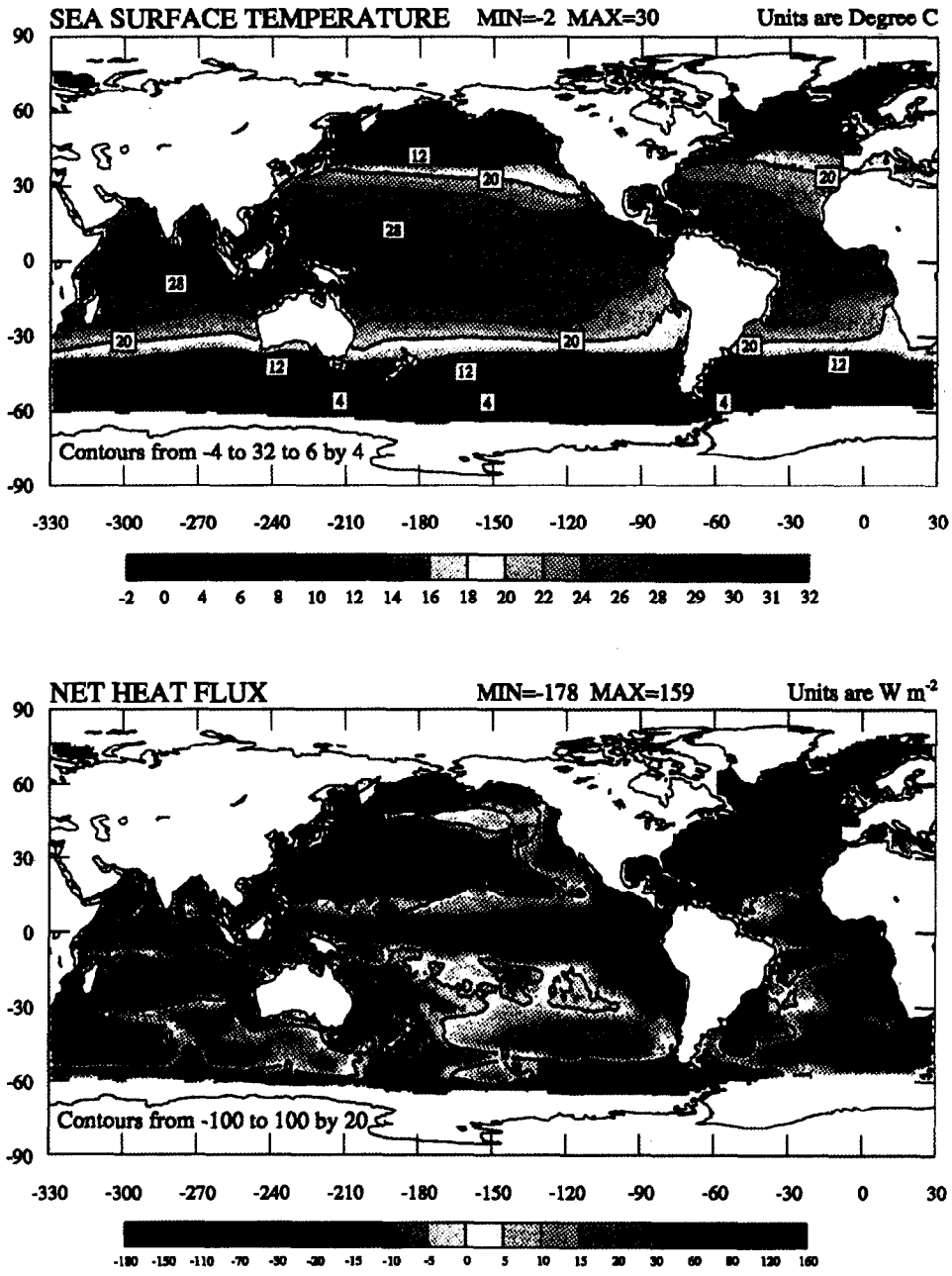

Fig. 1. Climatological annual mean of the SST in °C (top), and the net heat flux in $W \cdot m^{-2}$ (bottom), estimated from 3 years of ECMWF analyses (1986–1988). White areas over high latitude oceans indicate the presence of sea-ice.

surface wind stress, the latent and sensible surface heat fluxes, and the net short-wave and net long wave radiative heat fluxes during the first 6 hours of the forecast. ECMWF fluxes are therefore consistent with other ECMWF atmospheric surface variables through the parameterisation of the planetary boundary layer.

All ECMWF surface variables and fluxes are available on a grid of 1.125° longitude by 1.125° latitude, every six hours over a period of 5 years (1986–1990). The data base is currently being updated with data for the years 1991 and 1992.

A brief study of the 5-year mean climatology of the heat fluxes (Siefridt and Barnier, 1993) revealed an unrealistic increase in solar radiation in 1989 and 1990, concomitant with the use in the ECMWF model of a new parameterisation scheme for radiative fluxes and cloud optical properties (ECMWF, 1993). As a result, the 5-year mean net heat flux shows quite unrealistic values in areas of strong loss to the atmosphere (for example, in the Gulf Stream area the maximum heat loss is 140 W m^{-2} instead of the 200 W m^{-2} showed by most climatologies derived from VOS data). The zonally integrated heat transports for the various oceans also show unrealistic features for the years 1989 and 1990. Therefore, it is possible that systematic errors are present in the calculations of the heat fluxes for those two years of the analyses. Consequently, the present study only uses the first 3 years of the data set (1986–1988).

For every variable of the ECMWF data set, the 6-hour values have been averaged in time over year 1986, 1987 and 1988, to produce a climatological annual cycle (made up of a monthly mean for each calendar month), and a climatological annual mean (the total 3-year average). This climatology will be used in the calculations presented in the present paper. Note that the 6-hour scalar wind speed calculated as the modulus of the 6-hour wind vector is used to estimate the climatological scalar wind speed U_{10}. This value of the wind speed, which is different from that obtained as the modulus of the climatological wind vector, is the correct one to use in bulk formulas used to estimate the air–sea fluxes, and is thus used in the calculations of the thermal forcing in the following sections. Hanawa and Toba (1987) showed that using such a scalar average wind speed in the calculation of climatological estimates of the turbulent heat fluxes, reduces the errors arising from averaging the parameters involved in the bulk formulas to a level comparable to the errors induced by the uncertainties in the values of the turbulent heat transfer coefficients. Therefore, we made no corrections to the calculations of the thermal boundary condition which is developed in the following.

The climatological annual mean sea-surface temperature (SST) is shown in Fig. 1a. Temperatures below the freezing point of sea water ($-2°$ C) may be considered as indicative of areas of seasonal or permanent sea ice and are not plotted. The oceanic fronts of the major subtropical gyres (Gulf-stream and Kuroshio) and in the Antarctic Circumpolar Current (ACC) are well marked and exhibit larger meridional gradients than in most climatologies (Levitus, 1982). Maximum SST values (between 28 and 30° C) are found in the equatorial eastern Indian and western Pacific Oceans. Temperatures in the ACC range between 0 and 14° C.

The climatological mean net heat flux Q_{NET} is shown in Fig. 1b, with the convention of positive values presenting a heat gain for the ocean. The flux is not plotted in high latitude areas where the climatological SST is below $-2°$ C, because ECMWF fluxes are not representative of air–sea exchanges due to the presence of sea-ice. Patterns of ECMWF flux compare well with other climatologies from VOS observations (Esbensen and Kushnir, 1981; Hsiung, 1986; Oberhuber, 1988), and previous ECMWF climatologies (Simonot and Le Treut, 1987; Barnier and Simonot, 1990). The major subtropical gyres show considerable heat loss to the atmosphere (180 $W \cdot m^{-2}$ in the Gulf Stream, over 120 in the Kuroshio, and around 80 $W \cdot m^{-2}$ in the Aghulas, East Australian and Brazil currents). The greatest heat gains are found in the areas of strong upwelling (100 $W \cdot m^{-2}$ in the eastern Equatorial Pacific, 40 to 60 $W \cdot m^{-2}$ in the coastal regions of California, Portugal and Senegal, and over 100 $W \cdot m^{-2}$ off Peru and Angola).

These values are in agreement with most cli-

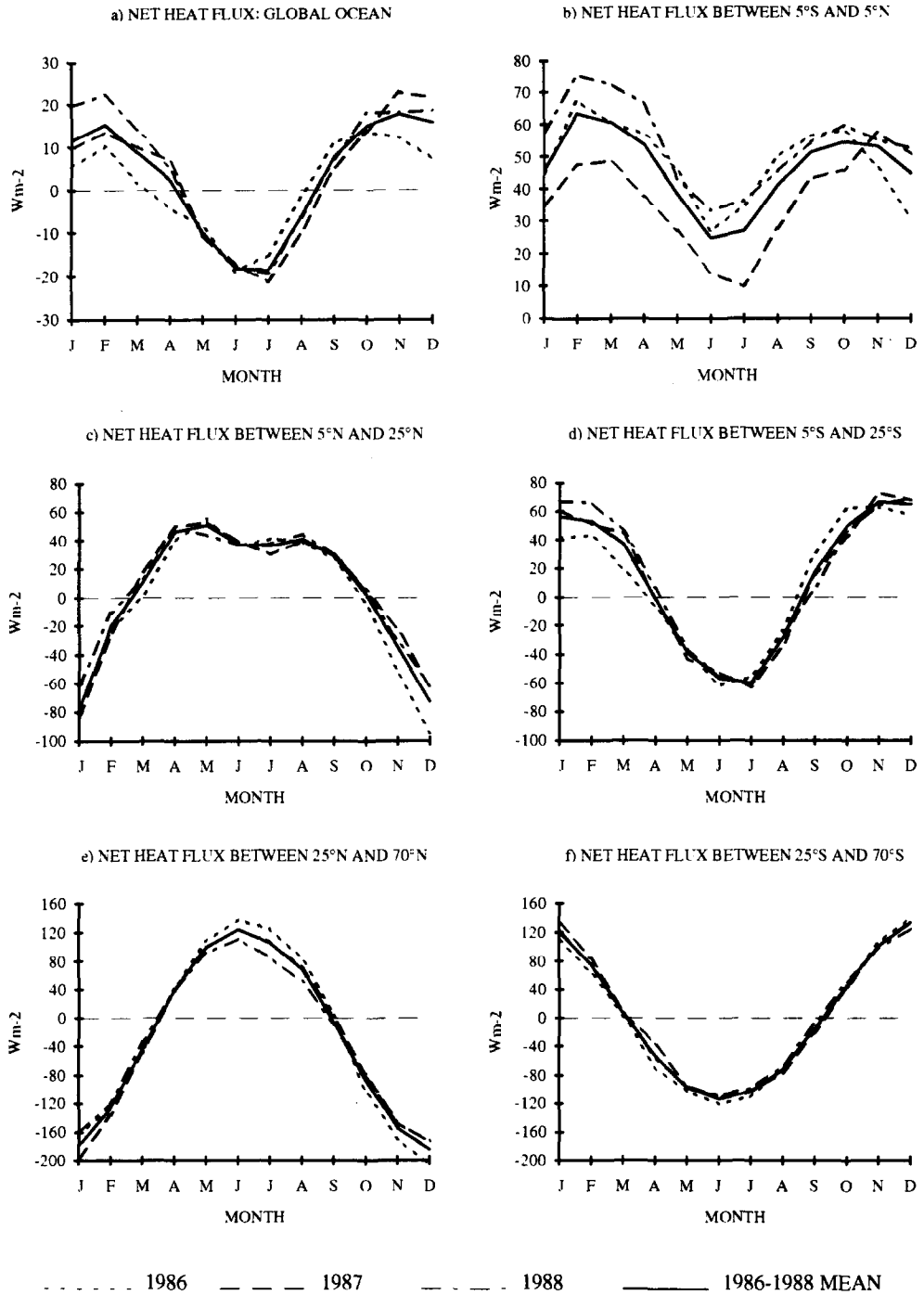

Fig. 2. Monthly mean variations of ECMWF net heat flux over the oceans, integrated over various bands of latitude, for 1986 (dotted line), 1987 (dashed line) and 1988 (dashed–dotted line). The three year average is also plotted (full line). Units are $W \cdot m^{-2}$.

matological estimates within 10 to 20%, the best quantitative agreement being with the climatology of Hsiung (1986). However, as already noted by Barnier and Simonot (1990), in areas of smaller values (under 20 $W \cdot m^{-2}$), discrepancies may be large enough to make the sign of the heat exchange uncertain. For example, in the center of the South Atlantic gyre the estimate given by ECMWF is positive (below 20 $W \cdot m^{-2}$) which prevents the areas of heat loss of the Aghulas and Brazil currents from joining, whereas in the climatology of Bunker (1988) these two regions are connected by a band of small negative flux (-5 $W \cdot m^{-2}$).

The three year period 1986–1988 includes the 1987 El Niño and the 1988 La Niña, events that can be noticed on the plots in Fig. 2 which show the monthly variation of the zonally averaged net heat flux for various latitude bands. At the Equator (Fig. 2b), the net heat flux in 1986 is very close to the 1986–1988 mean until November when it begins to drop below average. From November '86 to October '87, the flux remains 15 $W \cdot m^{-2}$ below average. This period corresponds to the 1987 El Niño, when the warming of the Equatorial Pacific Ocean induces a reduction of the heat flux from the atmosphere to the ocean. The La Niña event begins at the end of 1987, and reaches a maximum in the winter of 1988. Over that period, the anomalous cooling of the Equatorial Pacific results in an increase of heat gain by the ocean and the net heat flux is above normal. By the end of 1988, the situation appears to be back to average. At tropical and higher latitudes (Fig. 2c–f), the deviation from the mean is generally small (below 10 $W \cdot m^{-2}$), except in the southern tropics (Fig. 2d) from January to April, and at high latitudes in the Northern Hemisphere (Fig. 2e) during the summer (values close to 15 $W \cdot m^{-2}$). Therefore, the 1986–1988 mean net heat flux appears to be representative of the mean air–sea exchanges over that period, except in the intertropical band. There, the heat flux anomalies, due to warming (in 1987) followed by cooling (in 1988) of the upper Pacific Ocean, have opposite signs and have no significant effect on the three year average of the net heat flux. As seen before in the comments for Fig. 1b, this latter quantity is in rather good agreement with long term climatologies, although a three year period is rather short to be representative of a climate state.

3. Formulation of the thermal forcing

In this section, a formulation is proposed for a thermal boundary condition that ought to drive an ocean model toward a state of equilibrium with a prescribed climatological atmosphere which may include a seasonal cycle. Following Haney (1971) and Han (1984), the coupling between the atmosphere and the ocean model takes place through the flux at the air–sea interface. The hypothesis of a steady climatological atmosphere above the ocean implies that changes in the state of the ocean will induce changes in the surface fluxes only, in such a way that the ocean model will be pulled toward a state of "quasi-equilibrium" consistent with the prescribed atmosphere. We assume that after the ocean reaches that state, the difference between the model surface temperature T_S and the climatological sea surface temperature T_S^{clim} consistent with the prescribed atmosphere should be small.

Therefore, we may expand the dependence of the net heat flux on T_S in a truncated Taylor series about T_S^{clim}:

$$Q_{NET}(T_S) = Q_{NET}(T_S^{clim}) - \left(\frac{\partial Q_{NET}}{\partial T}\right)_{T_S^{clim}} (T_S^{clim} - T_S) \qquad (3)$$

with the convention of using positive values for heat gains. In this formulation, the model heat flux appears as the sum of two components: a prescribed climatological flux, the estimate for which can be provided by numerical weather prediction centers such as ECMWF and a correction term proportional to the difference between the climatological SST and the model surface temperature.

All climatological variables are prescribed and known from ECMWF analyses. The prescribed climatological flux $Q_{NET}(T_S^{clim})$ and the climatological sea surface temperature T_S^{clim} are those shown in Fig. 1.

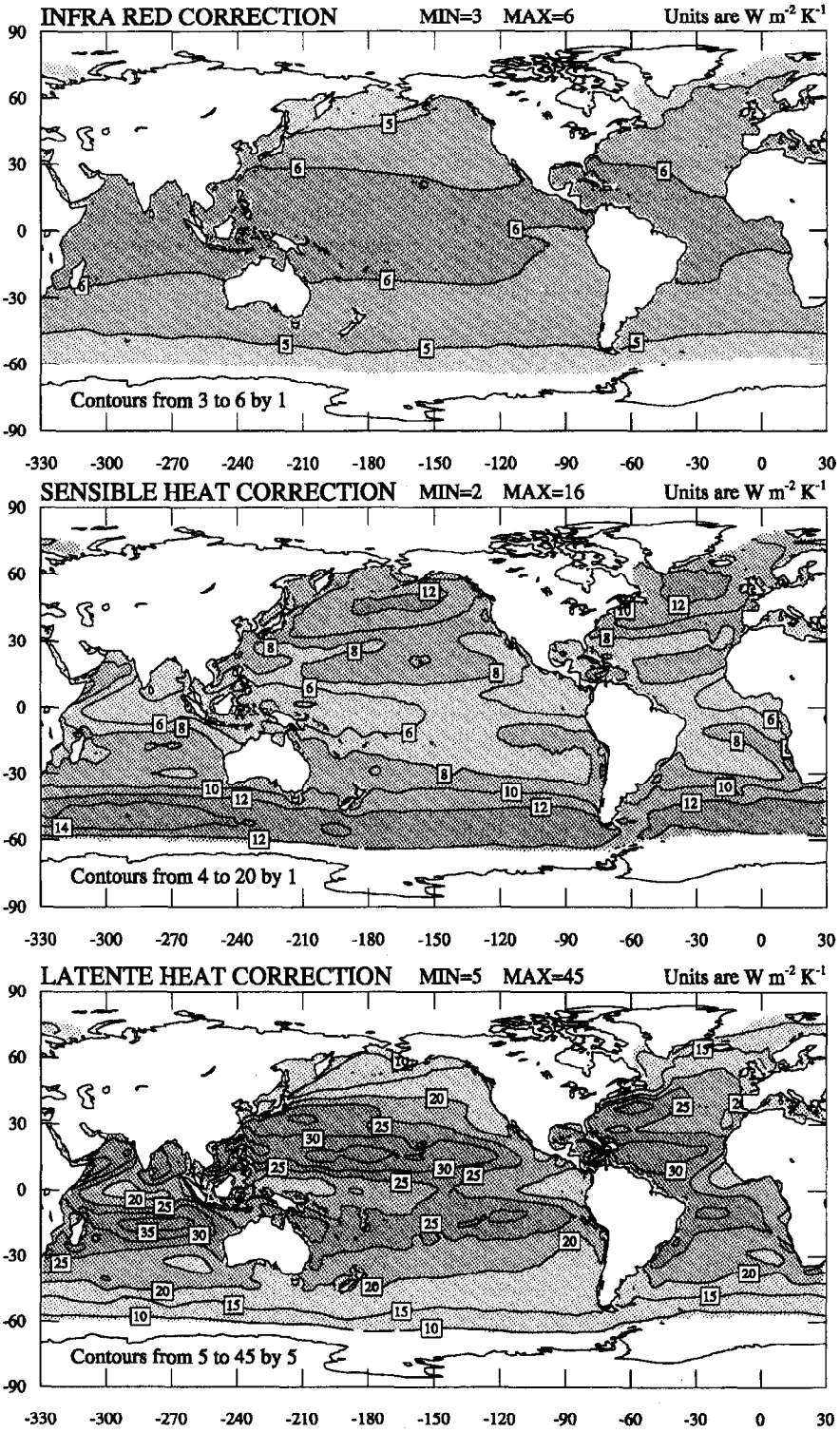
INFRA RED CORRECTION MIN=3 MAX=6 Units are W m-2 K-1
Contours from 3 to 6 by 1
SENSIBLE HEAT CORRECTION MIN=2 MAX=16 Units are W m-2 K-1
Contours from 4 to 20 by 1
LATENTE HEAT CORRECTION MIN=5 MAX=45 Units are W m-2 K-1
Contours from 5 to 45 by 5
90
60
30
0
-30
-60
-90
-330 -300 -270 -240 -210 -180 -150 -120 -90 -60 -30 0 30

To compute the net heat flux during the time-integration of an ocean model, it would be necessary to evaluate the correction term, and therefore to calculate the relaxation coefficient which depends upon climatological variables:

$$\left(\frac{\partial Q_{\mathrm{NET}}}{\partial T}\right)_{T_S = T_S^{\mathrm{clim}}} \tag{4}$$

The net heat flux Q_{NET} is obtained by adding of four components: solar radiation Q_S, infra-red radiation Q_{IR}, sensible heat flux Q_H and latent heat flux Q_E

$$Q_{\mathrm{NET}} = Q_S + Q_{\mathrm{IR}} + Q_H + Q_E$$

The following subsections describe how the contribution of each flux component in the relaxation coefficient is formulated from empirical formulas, and provide climatological estimates of each component obtained from the ECMWF climatology for 1986–1988.

3.1. Solar heat flux Q_S

In a prescribed climatological atmosphere, the net solar heat flux at the ocean surface should not depend on the model SST. The correction term is set to zero.

$$\frac{\partial Q_S}{\partial T} = 0$$

Therefore, the present formulation remains valid whether solar radiation is included in the net heat flux or is modelled with a penetration law.

3.2. Infra-red radiation Q_{IR}

The net long-wave radiation at the ocean surface is the sum of the downward radiation from the atmosphere and the upward radiation from the ocean surface. Under our hypothesis of a prescribed atmosphere, only the latter depends upon the ocean SST. Therefore, assuming the ocean radiates as a black body, we have:

$$\left(\frac{\partial Q_{\mathrm{IR}}}{\partial T}\right)_{T_S^{\mathrm{clim}}} = -4\sigma\left(T_S^{\mathrm{clim}}\right)^3 \tag{5a}$$

where $\sigma = 5.67 \cdot 10^{-8}$ $\mathrm{Wm^{-2}K^{-4}}$ is the Stefan–Boltzmann constant. We do not consider any return radiation from the clouds which is assumed to be independent of the ocean surface temperature. A climatological estimate of this term is calculated from the 3-year mean ECMWF climatology. It shows a zonal distribution and small amplitudes, from 3 $\mathrm{W \cdot m^{-2}K^{-1}}$ at high latitudes to 6 $\mathrm{W \cdot m^{-2}K^{-1}}$ in equatorial and tropical regions (Fig. 3a).

3.3. Sensible heat flux Q_H

The bulk formulation of the sensible heat flux at the sea surface is

$$Q_H = \rho_A C_P C_H U_A (T_A - T_S).$$

Notations are given in the Appendix. The contribution of the sensible heat flux to the correction term is

$$\left(\frac{\partial Q_H}{\partial T}\right)_{T_S^{\mathrm{clim}}} = -\rho_A C_P C_H U_A \tag{5b}$$

This term is proportional to the wind speed over the ocean. The climatological 3-year mean estimate of the correction due to sensible heat (Fig. 3b) is the greatest in areas of strong winds (westerlies in the ACC and at the northern edge of the subtropical gyres along the storm track, easterlies in the tropics), where it reaches values from 8 to 16 $\mathrm{W \cdot m^{-2}\ K^{-1}}$. In areas of low wind speed along the equator, where bulk formulas probably underestimate the turbulent exchanges, values are generally between 4 and 8 $\mathrm{W \cdot m^{-2}\ K^{-1}}$.

Fig. 3. Climatological annual mean of the various flux correction terms estimated from 3 years of ECMWF analyses (1986–1988). Infra-red radiations (top), sensible heat (middle) and latent heat (bottom). Units are $\mathrm{W \cdot m^{-2}K^{-1}}$. White areas over high latitude oceans indicate the presence of sea-ice.

3.4. Latent heat flux Q_H

The bulk formulation of the latent heat flux is

$$Q_E = -\rho_A C_E L U_A (q_s - q_A).$$

Notations are given in the Appendix. The atmosphere being steady, the correction term will only depend on the variation with T_S of the saturated specific humidity q_S:

$$\frac{\partial Q_E}{\partial T} = -\rho_A C_E L U_A \frac{\partial q_S}{\partial T}$$

(The correction induced by the dependency of latent heat L on T_S is almost two orders of magnitude smaller and is not taken into consideration). An expression of q_S can be given by

$$q_S(T) = \frac{0.622}{P_A} e_s(T)$$

where the saturated water pressure vapor is given by the Clausius–Clapeyron integrated law:

$$e_S(T) = 10^{(9.4051 - \frac{2353}{T})}$$

which yields the correction term:

$$\left(\frac{\partial Q_E}{\partial T}\right)_{T_S^{clim}} = -\rho_A C_E L U_A \cdot 2353 \ln 10 \cdot \frac{q_S(T_S^{clim})}{(T_S^{clim})^2} \quad (5c)$$

The correction for latent heat is the largest off all the correction terms. Its 3-year mean estimate from ECMWF climatology is shown in Fig. 3c. In the tropics, it can be three times larger than the correction due to sensible heat. The importance of the wind field in the evaporation process is clear. At the Equator for instance, the spatial patterns of lower latent heat correction closely follow those of low wind speed (Fig. 3b). However the dependency of the saturated air specific humidity on the SST has a significant impact on the amplitudes, which are the largest (30–40 $W \cdot m^{-2}K^{-1}$) in the tropics, and are still large (20 $W \cdot m^{-2}K^{-1}$) in equatorial regions. At mid-latitudes, this term is comparable to the correction term for sensible heat (6–18 $W \cdot m^{-2}\ K^{-1}$).

4. The surface thermal boundary condition

Whichever formulation is used to model the thermal forcing of an ocean GCM [the flux boundary condition (Eq. 1b) or the body force parameterisation (Eq. 2c)], the estimate of the heat flux could be written in the following form:

$$Q(T_S) = Q_1 + Q_2 \cdot (T_S^{clim} - T_S) \quad (6a)$$

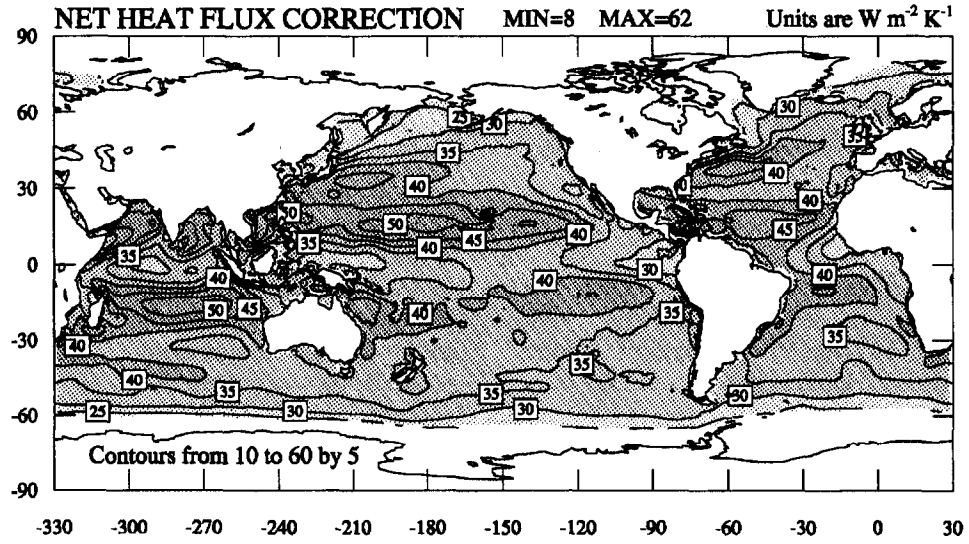

Fig. 4. Climatological annual mean of the total (net) heat flux correction term, estimated from 3 years of ECMWF analyses (1986–1988). Units are $W \cdot m^{-2}K^{-1}$. White areas over high latitude oceans indicate the presence of sea-ice.

with

$$Q_2 = -\left(\frac{\partial Q_{\mathrm{NET}}}{\partial T}\right)_{T_S^{\mathrm{clim}}}$$

$$= 4\sigma\left(T_S^{\mathrm{clim}}\right)^3 + \rho_A C_P C_H U_A + \rho_A C_E L U_A \cdot 2353 \ln 10 \cdot \frac{q_S\left(T_S^{\mathrm{clim}}\right)}{\left(T_S^{\mathrm{clim}}\right)^2}. \quad (6b)$$

If a penetration law is used for the solar heating as in (1a), Q_1 will be the climatological non solar heat flux $Q_{\mathrm{NS}}(T_S^{\mathrm{clim}})$ used in the surface flux boundary condition Eq. (1b). If not, Q_1 will be the climatological net heat flux $Q_{\mathrm{NET}}(T_S^{\mathrm{clim}})$.

Q_2 quantifies the variations of the surface heat flux according to the variations of the model ocean surface temperature over the climatological SST. A 3-year mean climatological estimate of the correction term Q_2, calculated from the ECMWF data set, is shown in Fig. 4. It represents the addition of the features shown in Fig. 3 and exhibits a pattern which is most influenced by the latent heat flux, with large values in tropical areas (40–60 $\mathrm{W \cdot m^{-2}K^{-1}}$) and mid-latitude gyres (30–50 $\mathrm{W \cdot m^{-2}K^{-1}}$). Smaller values are found along the 30° latitude line in each hemisphere because of lower wind speed conditions. The flux correction is below 35 $\mathrm{W \cdot m^{-2}K^{-1}}$ along most of the equator. In these areas the flux correction is probably underestimated because of the use of bulk formulas in low wind speed conditions. Small corrections are also found at high latitudes.

Understanding of the impact of the correction term on the model thermal forcing is straightforward. In the tropics, an increase by 1 K of the model SST over the climatological SST will produce a flux correction Q_2 of the order of -50 $\mathrm{W \cdot m^{-2}K^{-1}}$. The heat flux that forces the model will consequently be reduced which will tend to pull the model SST toward the prescribed climatological value. In the subtropical gyres of the northern hemisphere, a variation of 1 K in model SST will produce a heat flux correction close to 40 $\mathrm{W \cdot m^{-2}K^{-1}}$.

The correction term $Q_2 \cdot (T_S^{\mathrm{clim}} - T_S)$ is similar to that of Haney (1971) and Han (1984), expressed in terms of the climatological SST. In Haney's as well as in Han's formulations, it is assumed that the model SST is close to the surface air temperature, and the model heat flux (Eq. 3) is expanded about the air temperature. Consequently, the correction term is expressed in terms of the surface air temperature, and in Eq. (6a) Q_1 does not include the sensible heat flux since this is totally treated in the correction term. Thus the sensible heat flux is zero when the surface air temperature is equal to the ocean SST.

In the present case, it is hypothesized that the climatological atmosphere is in equilibrium with an ocean where the SST is the climatological ocean surface temperature T_S^{clim}. Therefore, the model heat flux has been expanded about T_S^{clim} in order to obtain a surface heat flux equal to the climatological heat flux in the case where the model SST is equal to T_S^{clim}. Consequently, T_S^{clim} is the climatological variable that governs the correction term Q_2, and Q_1, the part of the surface heat flux that does not depend on the model SST, includes the sensible heat flux.

A qualitative comparison with Han's climatological estimate of Q_2 shows significant similarities in the large-scale patterns: the large values of Q_2 are found in all tropical oceans and major subtropical gyres, and lower values are found along the 30° latitude line in each Hemisphere and along the Equator. Quantitatively the magnitude of the flux correction provided by the ECMWF climatology is less than that given by Han's calculations. The ECMWF estimate of Q_2 shows values ranging from 20 to 65 $\mathrm{W \cdot m^{-2}K^{-1}}$ whereas Han's estimate ranges from 35 to 70 $\mathrm{W \cdot m^{-2}K^{-1}}$. The greatest differences (10–15 $\mathrm{W \cdot m^{-2}K^{-1}}$) are noticed in the areas of low wind speed (equatorial and 30° latitude bands). In the subtropical gyres, ECMWF estimates are lower by 5 $\mathrm{W \cdot m^{-2}K^{-1}}$. Tropical maximum values have equivalent amplitudes (close to 60 $\mathrm{W \cdot m^{-2}K^{-1}}$) in both analyses. These quantitative differences have two origins: the different nature of the data sets that are used and the slightly different formulations (as stated above, the sensible heat flux is treated entirely as a correction term in Han's formulation).

Haney (1971) gives another interpretation of the formulation of the model surface heat flux. Eq. (6a) can be written in the following form:

$$Q_{\mathrm{NET}}(T_{\mathrm{S}}) = Q_2(T_{\mathrm{A}}^* - T_{\mathrm{S}}) \tag{7a}$$

with T_{A}^*, being an "apparent" air temperature, defined as:

$$T_{\mathrm{A}}^* = T_{\mathrm{S}}^{\mathrm{clim}} + \frac{Q_1}{Q_2} \tag{7b}$$

If such a formulation is used to estimate the thermal forcing Eq. (2c), the temperature Eq. (2a) will become

$$\frac{\partial T}{\partial t} = \text{Advection} + \text{Diffusion} + \frac{1}{R_T}(T_A^* - T) \tag{8a}$$

where the characteristic relaxation time scale R_T is

$$R_T = \frac{\rho_0 C_{Pw} \Delta z}{Q_2} \tag{8b}$$

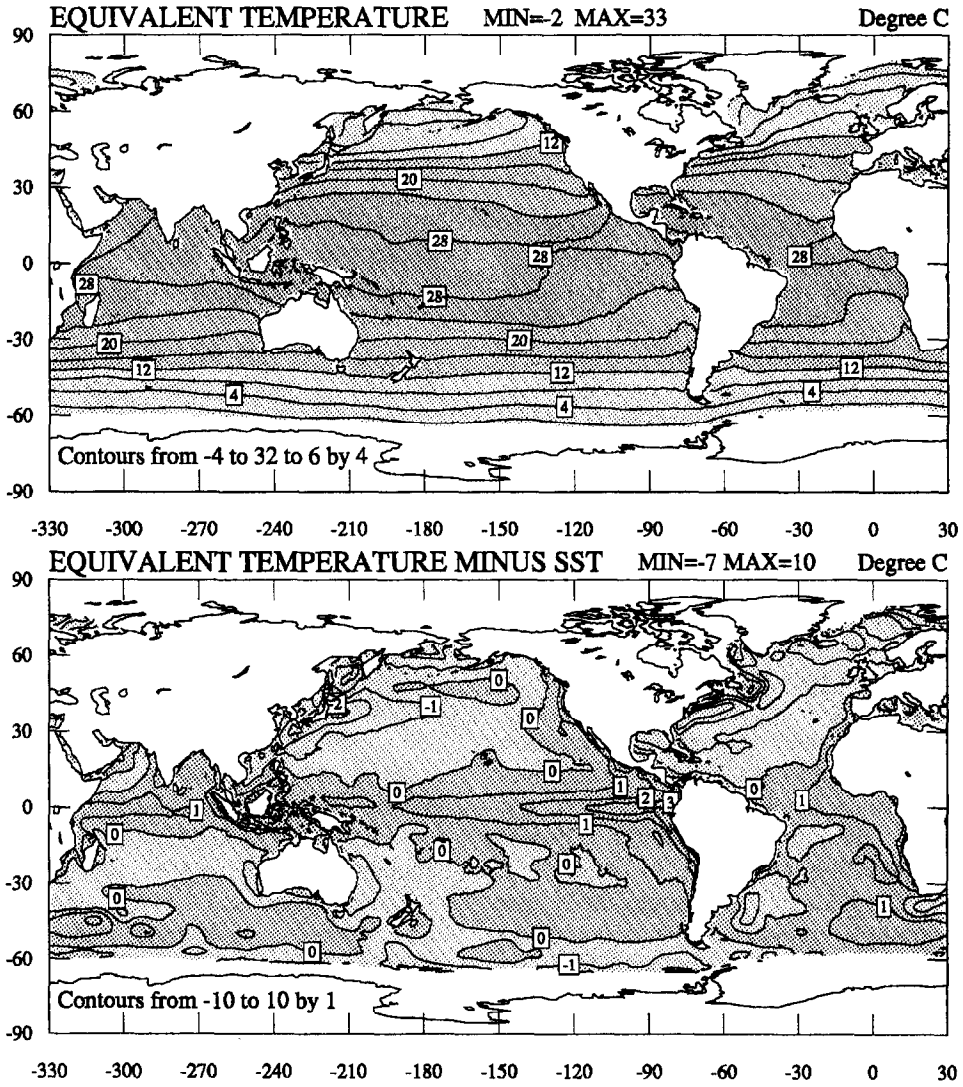

Fig. 5. Climatological mean of the apparent air temperature (top), and its difference with the climatological mean SST (bottom), estimated from 3 years of ECMWF analyses (1986–1988). Units are °C. White areas over high latitude oceans indicate the presence of sea-ice.

where Δz is the Ekman layer depth, set to 35 m in the present calculations. Eq. (8a) shows that the thermal forcing of the model can be formulated as a relaxation of the model ocean surface temperature toward an apparent air temperature T_A^* which includes the effects of the heat exchanges at the air–sea interface.

The ECMWF 3-year climatology of T_A^* and its difference with the climatological ocean surface temperature T_S^{clim} are shown in Fig. 5. The apparent air temperature shows a pattern similar to that of the climatological SST, but significant differences are noticed in key regions. T_A^* is significantly colder over most of the subtropical gyres of the northern hemisphere, and is warmer in the tropical bands (from 10 N to 10 S). The subtropical gyres of the Southern Hemisphere also exhibit colder apparent air temperatures on their western side. The South Atlantic appears as a special case since it has warmer apparent air temperatures almost everywhere except over the Brazil current and the retroflection of the Aghulas current. In the ACC, T_A^* is generally warmer than the climatological SST, except in the southern Pacific.

In major western boundary currents, T_A^* is colder by an amount of 2° C to 3° C, reflecting the large heat loss from the ocean to the atmosphere. Equatorial regions are warmer by 1° C to 2° C. The fact that T_A^* reflects the air–sea exchanges is clearly shown in the map of the difference with T_S^{clim} (Fig. 5b), the spatial pattern of which is similar to that of the net heat flux shown in Fig. 1.

The climatological estimate of T_A^*, calculated by Han (1984) agrees, at the large scale, with that presented in Fig. 5a. Values above 30° C are found in the Equatorial Indian and Western Pacific, while values above 28° C are found in the Equatorial Atlantic. The global patterns are similar. However, Han's temperatures appear colder at high latitudes (the 8° C isotherm is further north).

The climatological estimate of the relaxation coefficient R_T is shown in Fig. 6. Since R_T is inversely proportional to the flux correction Q_2 (Fig. 3), it presents similar patterns and shows shorter relaxation time-scales where the flux correction is large. This plot provides a quantification of the relaxation according to geographical areas. A flux correction of 40 to 50 $W \cdot m^{-2}$ in tropical regions means a relaxation time-scale of 35 to 40 days, a value commonly used in OGCM simulations. In subtropical gyres this constant

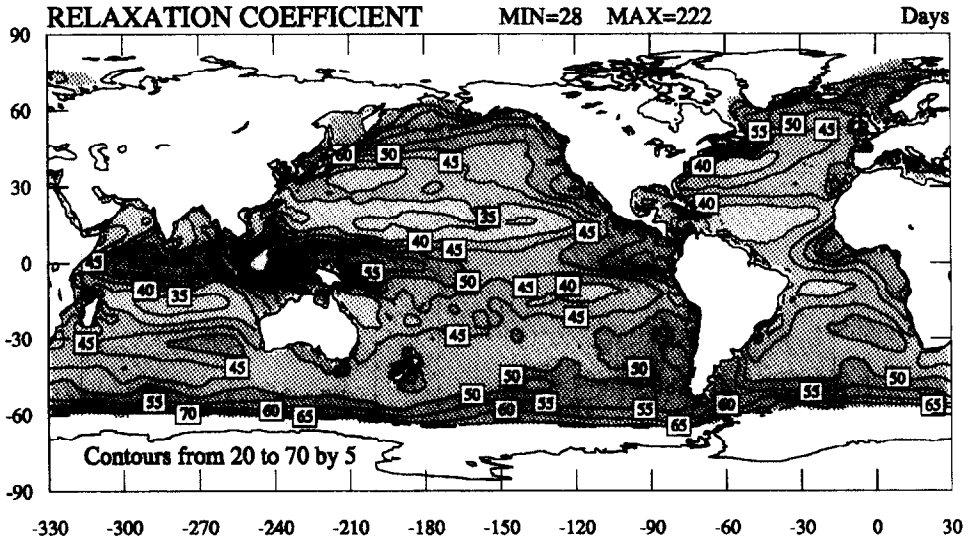

Fig. 6. Estimate of the relaxation constant corresponding to the total (net) heat flux correction shown in Fig. 3. Units are days. White areas over high latitude oceans indicate the presence of sea-ice.

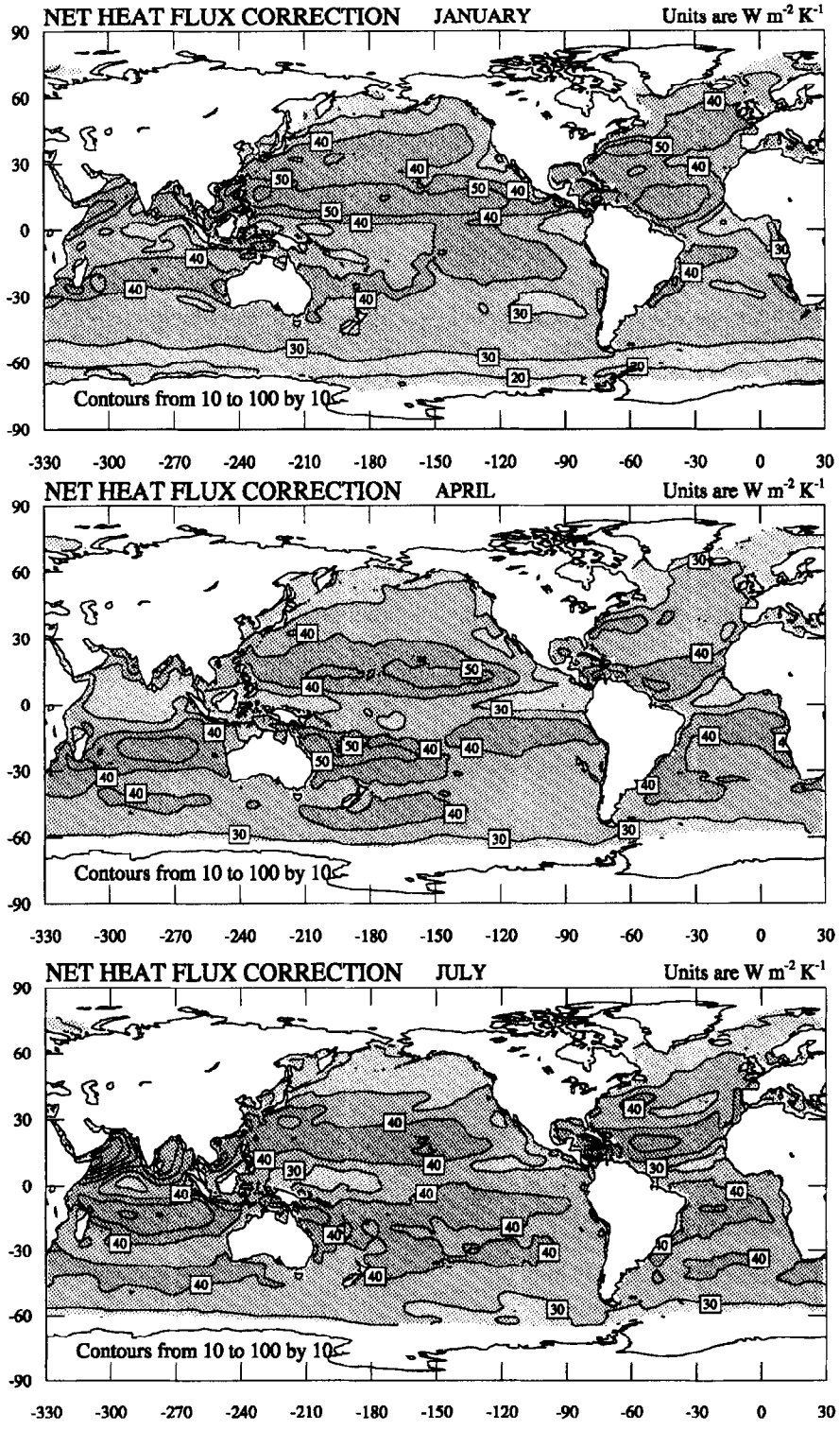
NET HEAT FLUX CORRECTION JANUARY
Units are W m-2 K-1
Contours from 10 to 100 by 10
NET HEAT FLUX CORRECTION APRIL
Units are W m-2 K-1
Contours from 10 to 100 by 10
NET HEAT FLUX CORRECTION JULY
Units are W m-2 K-1
Contours from 10 to 100 by 10
90
60
30
0
-30
-60
-90
-330 -300 -270 -240 -210 -180 -150 -120 -90 -60 -30 0 30

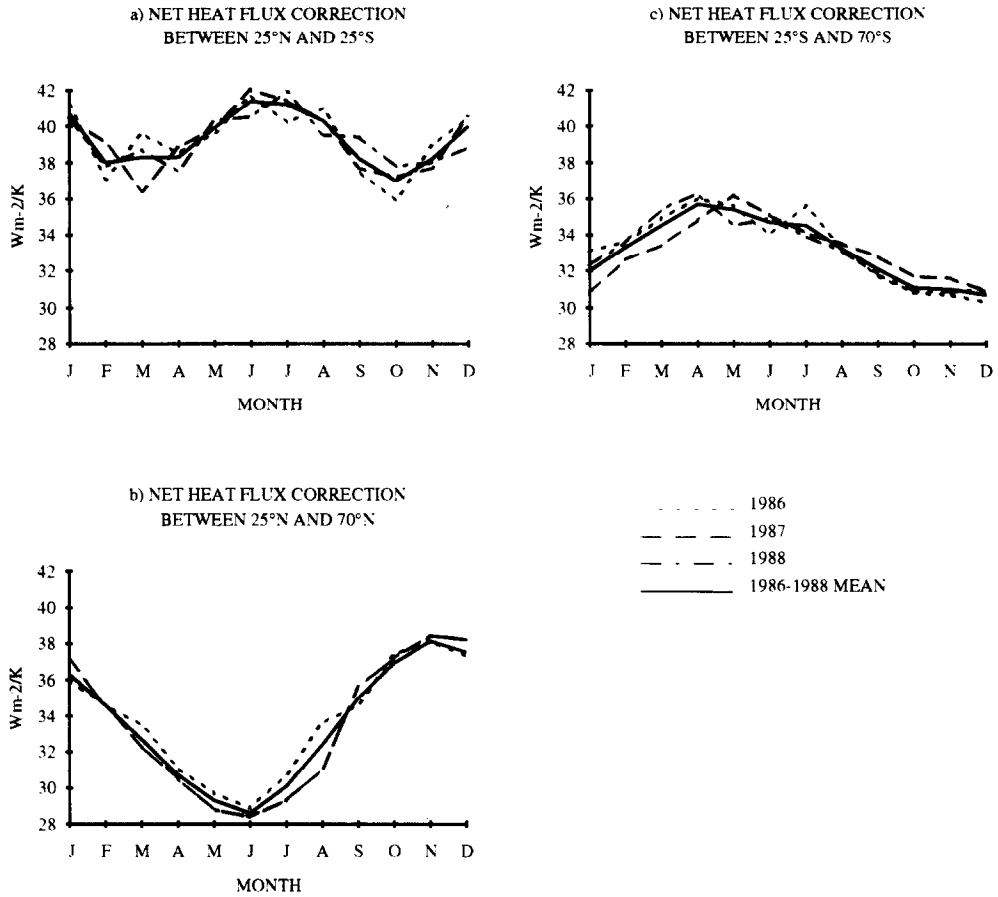

Fig. 8. Monthly mean variations of the heat flux correction Q_2, integrated over various bands of latitude, for 1986 (dotted line), 1987 (dashed line) and 1988 (dashed–dotted line). The three year average is also plotted (full line). Units are $W \cdot m^{-2}K^{-1}$.

gradually varies from west to east from 40 to 60 days, but varies very rapidly (from 40 to 70 days) across the Gulf Stream and the Kuroshio. The separation between the tropics and mid-latitudes is marked by relatively higher values of the relaxation constant (around 40 days). In the equatorial band, R_T shows values of 45 to 60 days, but a correction for low wind speed in the bulk formulas (Godfrey and Beljaars, 1991) would probably give smaller values. In the ACC, R_T increases rapidly from north to south, from 50 to 70 days.

5. Seasonal cycle

This section briefly investigates the seasonal variations of the flux correction term as defined in Eq. (6b). Fig. 7 shows the climatological monthly mean of this term for three different months representative of various seasons: January, April and July. The values of the flux correction in the Arctic Ocean are not considered because the ice coverage is not well defined. In Fig. 7c (July mean) the ice coverage in the Arctic

Fig. 7. Climatological monthly mean for January (top), April (middle) and July (bottom) of the total (net) heat flux correction term, estimated from 3 years of ECMWF analyses (1986–1988). White areas over high latitude oceans indicate the presence of sea-ice. Units are $W \cdot m^{-2}K^{-1}$.

has been determined from the seasonal climatology of the 0.5° C SST. This value has been chosen instead of that of −2° C (close to the freezing point of sea water) used for all the other figures, because in summer the surface temperature provided by ECMWF analyses over the ice of the Arctic is close to and sometimes above zero.

The largest seasonal variations are obviously found where the monsoon cycle is the dominant signal: the Indian Ocean. There, the flux correction is 50 $W \cdot m^{-2}K^{-1}$ during the winter monsoon, below 30 $W \cdot m^{-2}K^{-1}$ during the transition periods, and over 80 $W \cdot m^{-2}K^{-1}$ during the summer monsoon. In areas not influenced by the monsoon regime, the pattern of the flux correction does not show drastic seasonal variations, and the pattern of the various monthly means globally follows that of the annual mean. Little variability is found in the tropical band (including the equator) and in the ACC. The changes observed from one season to another mostly concern the subtropical gyres, where the amplitude of the flux correction is larger by almost 20 $W \cdot m^{-2}K^{-1}$ during the winter.

Fig. 8 shows the seasonal variations of the flux correction for various latitude bands. In the inter-tropical band (Fig. 8a), a semi-annual oscillation of small amplitude (4 $W \cdot m^{-2}K^{-1}$, or 10% of the annual mean) is apparent. At mid-latitudes in both Hemispheres (Fig. 8b, c), the flux correction shows an annual oscillation, with a maximum correction during the respective winters. The amplitude of the oscillation is significant in the Northern Hemisphere (10 $W \cdot m^{-2}K^{-1}$, over 1/4 of the annual mean value), and less pronounced in the Southern Hemisphere (5 $W \cdot m^{-2}K^{-1}$, less than 1/6 of the annual mean). The year to year variations are small, generally of the order of 1 $W \cdot m^{-2}K^{-1}$.

6. Conclusion

We have defined and analysed a surface thermal boundary condition for a global ocean model. Our formulation is based on previous methods which have used a flux correction to allow for a feedback from the ocean to the atmosphere which remains in a climatological state. The flux correction varies according to the model SST, which gives the model an essential degree of freedom in its determination of heat transport. The definition of the flux correction term is based on bulk formulas, so that air–sea exchanges are explicitly accounted for in the heat forcing, as long as the correction term does not become the major forcing.

The thermal forcing (heat flux and correction term) is estimated from a 3-year climatology of atmospheric surface fields given by the 6-hour analyses of ECMWF. The climatological net heat flux shows values which are within 10 to 20% of agreement with most climatological estimates. The analysis of the correction flux shows a significant variation in the amplitude of the correction with latitude, with the largest values (above 50 $W \cdot m^{-2}K^{-1}$) in tropical regions, minimum values (below 30 $W \cdot m^{-2}K^{-1}$) in areas of low wind speed along the Equator and at high latitudes, and large values again (50 $W \cdot m^{-2}K^{-1}$) in most subtropical gyres. Seasonal variations show the importance of the monsoon cycle in the Indian Ocean. However, the low values which appear in areas of low wind speed (the Equator and, to a lesser degree, along the 30 degree latitude line in both hemispheres) may result from an underestimation due to the use of bulk formulas to determine the analytical expression of the correction term. A correction for low wind speed could be used to solve this problem (Godfrey and Beljaars, 1991).

Finally, we believe that ocean GCM's should be forced with internally consistent forcings. Using the output of Atmospheric GCM's is a way to achieve this, since all fluxes are consistent through the surface boundary layer parameterisation used in the atmospheric GCM's. The way we defined our surface thermal boundary condition, which involves analysed surface fields from ECMWF, also ensures the internal consistency of the flux correction. Furthermore, a parameterisation of the fresh water flux based on precipitation and evaporation rates estimated from ECMWF analyses would then ensure the consistency between the thermal and salinity forcing of ocean models.

7. Appendix

Table 1
Definition of the various variables and parameters

Variable–Parameter	Symbol	Value–Units
Ocean model surface temperature	T_S	K
Climatological sea surface temperature	T_S^{clim}	K
Sea water density	ρ_0	1026 kg m^{-3}
Specific heat of sea water at constant pressure	C_{Pw}	4.18×10^3 J kg^{-1}K^{-1}
Air density	ρ_A	kgm^{-3}
Air specific heat at constant pressure	C_P	1.0048×10^3 J kg^{-1}K^{-1}
Bulk transfer coefficient for sensible heat	C_H	1×10^{-3}
Bulk transfer coefficient for latent heat	C_E	1.15×10^{-3}
Scalar wind speed at anemometer level	U_A	ms^{-1}
Air temperature at anemometer level	T_A	K
Latent heat of vaporisation	L	2.508×10^6 J kg^{-1}
Saturated air specific humidity	q_S	%
Air specific humidity at anemometer level	q_A	%
Mean sea level pressure	P_A	mb
Estimate of the Ekman Layer Depth	Δz	35 m

Acknowledgements

The authors are supported by the Centre National de la Recherche Scientifique and Ministère de l'Enseignement Superieur et de la Recherche. This research was funded by the Institut National des Sciences de l'Univers and IFREMER through the Programme National d'Etude de la Dynamique du Climat, (grant IFREMER 92 1430 055) and by the DYNAMO project of the European Union (grant MAS2-CT93-0060). Support for computations was provided by the Conseil Scientifique du Centre de Calcul Vectoriel pour la Recherche in Palaiseau (France). ECMWF analyses were made available by the AVISO vent-flux data base.

References

Barnier, B. and Simonot, J.Y., 1990. Mean and variability of the net surface heat flux over the North and the South Atlantic in 1985–1986 from day-one predictions of the ECMWF. J. Geophys. Res., 95: 13,301–13,311.

Bengtsson, L., Kanamitsu, M., Kallberg, P. and Uppala, S., 1982. FGGE 4-dimensional data assimilation at ECMWF. Bull. Am. Meteorol. Soc., 63: 29–43.

Bleck, R., Hanson, H.P., Hu, D., and Kraus, E.B., 1989. Mixed-layer–thermocline interaction in a three dimensional isopycnic model coordinate model, J. Phys. Oceanogr., 19: 1417–1439.

Böning, C.W. and Herrmann, P., 1994. Annual cycle of poleward heat transport in the ocean: results from high-resolution modeling of the North and Equatorial Atlantic. J. Phys. Oceanogr.: 24: 91–107.

Bunker, A., 1976. Computations of surface energy flux and annual air–sea interaction cycles of the North Atlantic Ocean. Mon. Weather Rev., 104: 1122–1240.

Bunker, A., 1988. Surface energy fluxes of the South Atlantic Ocean. Mon. Weather Rev., 116: 809–823.

Bryan, F.O. and Holland, W.R., 1989. A high resolution simulation of the wind- and thermohaline-driven circulation in the North Atlantic Ocean. In: P. Muller and D. Henderson (Editors), Parameterisation of Small Scale Processes. 'Aha Huilko'a Proc. Hawaiian Winter Workshop. Spec. Publ., 99-116 Hawaii Inst. Geophys.

Cox, M.C. and Bryan, K., 1984. A numerical model of the ventilated thermocline. J. Phys. Oceanogr., 14: 674–687.

ECMWF, 1993. The Description of the ECMWF/WCRP Level III-A Atmospheric Data Archive. Technical Attachment, 49 pp. ECMWF Shinfield Park, Reading, UK.

Esbensen, S.K. and Kushnir, Y., 1981. The Heat Budget of the Global Ocean: An Atlas based on Estimates from Surface Marine Observations. Climatic Res. Inst. Rep., 29. OSU, Corvallis, 27 pp.

Gaspard, P., Gregoris, Y. and Lefevre, J.M., 1990. A simple kinetic energy model for simulations of the oceanic vertical mixing: tests at station Papa and Long-Term Upper Ocean Study site. J. Geophys. Res., 95: 16,179–16,193.

Godfrey, J.S. and Beljaars, A.C.M., 1991. On the turbulent fluxes of buoyancy, heat and moisture at the air–sea interface at low wind speeds. J. Geophys. Res., 96: 22,043–22,048.

Han, Y.-J., 1984. A numerical world ocean general circulation model. Part II. A baroclinic experiment. Dyn. Atmos. Oceans, 8: 141–172.

Hanawa, K. and Toba, Y., 1987. Critical examination of estimation methods of long-term mean air–sea heat and momentum transfers. Ocean–Air Interactions, 1: 79–93.

Haney, R.L., 1971. Surface thermal boundary condition for ocean circulation models. J. Phys. Oceanogr., 1: 145–167.

Holland, W.R. and Bryan, F.O., 1994. Sensitivity studies on the role of the ocean in global change. In: P. Malanotte-Rizzoli and A.R. Robinson (Editors), Ocean Processes in Climate Dynamics: Global and Mediterranean Examples. Academic Publishers, the Netherlands, pp. 111–134.

Hsiung, J., 1986. Mean surface energy fluxes over the global ocean. J. Geophys. Res., 91: 10,585–10,606.

Huang, R.X., 1993. Real freshwater flux as a natural boundary condition for the salinity balance and thermohaline circulation forced by evaporation and precipitation. J. Phys. Oceanogr., 23: 2428–2446.

Lambert, S.J. and Boer, G.J., 1988. Surface Fluxes and Stresses in General Circulation Models. Canadian Climate Center, Rep., N88-1, CCRN18, 183 pp.

Levitus, S., 1982. Climatological Atlas of the World Ocean. NOAA Prof. Pap., 13. ERL, Geophysical Fluid Dynamics Laboratory, Princetown, N.J., 173 pp.

Moore, A.M. and Reason, C.J.C., 1993. The response of a global ocean general circulation model to climatological surface boundary conditions for temperature and salinity. J. Phys. Oceanogr., 23: 300–328.

Oberhuber, J.M., 1988. An Atlas based on the COADS Data Set: The Budget of Heat, Buoyancy and Turbulent Kinetic Energy at the Surface of the Global Ocean. Max-Plank-Institut für Meteorologie, Hamburg, Germany, 100 pp.

Paulson, C.A. and Simpson, J.J., 1977. Irradiance measurements in the upper ocean. J. Phys. Oceanogr., 7: 952–956.

Semtner, A.J. and Chervin, R.M., 1988. A simulation of the global ocean circulation with resolved eddies. J. Geophys. Res., 93: 15,502–15,522.

Semtner, A.J. and Chervin, R.M., 1992. Ocean general circulation from a global eddy-resolving model. J. Geophys. Res., 97: 5493–5550.

Siefridt, L. and Barnier, B., 1993. Banque de Données AVISO Vent/flux: Climatologie des Analyses de Surface du CEP-MMT, Rapp. IFREMER N° 91 1430 025, 43 pp.

Simonot, J.Y. and Le Treut, H., 1987. Surface heat fluxes from a numerical weather prediction system. Clim. Dyn., 2: 11–28.

Rosati, A. and Miyakoda, K., 1988. A general circulation model for upper ocean simulation. J. Phys. Oceanogr., 18: 1601–1626.

Takano, K., Mintz, Y. and Han, J.-Y., 1973. Numerical simulation of the world ocean circulation. 2nd Conf. Numerical Weather Prediction. Am. Meteorol. Soc., Monterey, CA.

Tziperman, E., Toggweiler, J.R., Feliks, Y. and Bryan, K., 1994. Instability of the thermohaline circulation with respect to mixed boundary conditions: Is it really a problem for realistic models? J. Phys. Oceanogr., 24: 217–232.

Weaver, A.J. and Sarachik, E.S., 1991. The role of mixed boundary condition in numerical ocean models of the ocean's climate. J. Phys. Oceanogr., 21: 1470–1493.

Webb, D.J. et al. (The FRAM Group), 1991. Using an eddy resolving model to study the Southern Ocean. EOS, 72(15): 169, 174, 175.